

Geocarto International



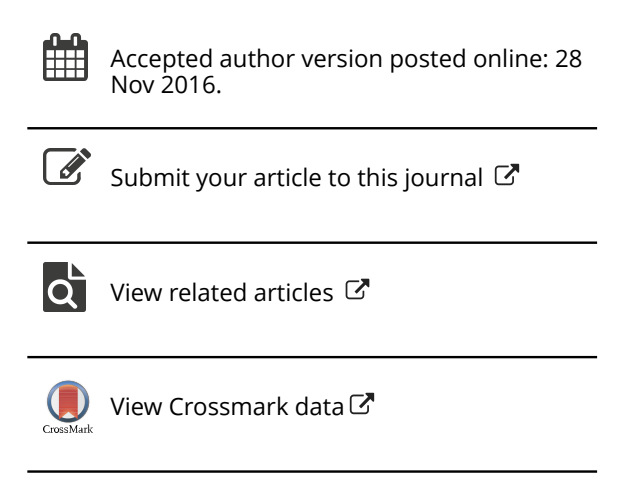
ISSN: 1010-6049 (Print) 1752-0762 (Online) Journal homepage: http://www.tandfonline.com/loi/tgei20

Remote Sensing of Nutrients in a Subtropical African Reservoir: Testing Utility of Landsat 8

Mhosisi Masocha, Chipo Mungenge & Tamuka Nhiwatiwa

To cite this article: Mhosisi Masocha, Chipo Mungenge & Tamuka Nhiwatiwa (2016): Remote Sensing of Nutrients in a Subtropical African Reservoir: Testing Utility of Landsat 8, Geocarto International, DOI: 10.1080/10106049.2016.1265596

To link to this article: http://dx.doi.org/10.1080/10106049.2016.1265596



Full Terms & Conditions of access and use can be found at http://www.tandfonline.com/action/journalInformation?journalCode=tgei20

Publisher: Taylor & Francis

Journal: Geocarto International

DOI: http://dx.doi.org/10.1080/10106049.2016.1265596

Remote Sensing of Nutrients in a Subtropical African Reservoir: Testing Utility of Landsat 8

Mhosisi Masocha^{a*}, Chipo Mungenge^b and Tamuka Nhiwatiwa^a

^aUniversity of Zimbabwe, Faculty of Science, Department of Geography & Environmental Science, Box MP 167, Mount Pleasant, Harare, Zimbabwe

^bUniversity of Zimbabwe, Faculty of Science, Department of Biological Sciences, Box MP 167, Mount Pleasant, Harare, Zimbabwe

*Corresponding Author Email: mmasocha@science.uz.ac.zw

Remote Sensing of Nutrients in a Subtropical African Reservoir: Testing Utility of Landsat

Abstract

Remote sensing is useful for water quality assessments but current remote sensing applications favor parameters that are easy to detect such as chlorophyll-a. An assessment of the utility of Landsat 8 for detecting nutrients was conducted in Mazvikadei reservoir in Zimbabwe. The main objective was to determine if nutrients often overlooked by remote sensing and yet are the main determinants of water quality can be remotely sensed. Sampling targeted ammonia, nitrates, and reactive phosphorus from May to October 2015. *In-situ* nutrient concentrations were regressed against reflectance derived from Landsat 8 imagery. Strong negative relationships were found between ammonia and the near infrared band in July ($R^2 = 0.80$, P < 0.05) as well as between nitrates and the blue band ($R^2 = 0.67$, P < 0.05) in June. Overall, the results suggest that the cool dry season is the optimum time to use Landsat 8 for monitoring nutrients in tropical lakes.

Keywords: ammonia, lake, monitoring, nitrates, reactive phosphorus, water quality

Introduction

Monitoring water quality in tropical African reservoirs has proved difficult due to lack of efficient and cost effective data collection systems. Remote sensing and Geographic Information Systems (GIS) are promising tools for assessing and monitoring water quality (Dekker et al. 1996). Unlike field based protocols that do not provide a synoptic view of water quality changes in water bodies, repeated measurements taken by sensors on satellite platforms permit regular monitoring of water quality at different spatial scales (Skidmore et al. 1997). However, much work still needs to be done to explore whether some of the recently launched medium spatial resolution sensors such as Landsat Operational Land Imager (OLI) are useful tools for providing reliable spatial information on water quality in tropical reservoirs in Africa. Given the scarcity of data on water quality in these systems on the continent, such work is needed to complement *insitu* field measurements from few scattered monitoring stations to inform water management (Usali and Ismail 2010).

The success of satellite based water quality monitoring is to a large extent dependent on careful selection of water quality parameters. Turbidity and chlorophyll-a are widely used parameters for characterizing the physico-chemical properties of reservoirs. From a remote sensing point of view, these two parameters have optical properties that make them amenable to measurement by satellite remote sensing thus giving a near-time picture of the environmental status of the target feservoir (Moore 1980). Turbidity measures light scattering in water due to suspended matter while chlorophyll-a is the substance responsible for the pigment of algal plants thus making it a good indicator of algal biomass in a water body (Duan et al. 2007).

Previous research has explored retrieval of chlorophyll-*a* from satellite images in marine and freshwater systems using different sensors such as the Sea-viewing Wide Field of view Sensor (SeaWiFS) (O'Reilly et al. 1998), Landsat Thematic Mapper (Ekstrand 1992), Medium Resolution Imaging Spectrometer (MERIS) (Gordoa et al. 2008, Matthews 2014), and Moderate Resolution Imaging Spectroradiometer (MODIS) (Binding et al. 2012). The spatio-temporal dynamics of turbidity have also been evaluated using optical data retrieved from MODIS-Aqua imagery (Ndungu et al. 2013).

One major advantage of using remote sensing over traditional field-based methods for water quality monitoring is that the former provides both spatial and temporal information of surface water characteristics (Dube et al. 2015). Thus, while *in-situ* measurements are considered to be fairly accurate, their common drawback is that they are often restricted to selected sampling points which implies that one cannot monitor the dynamics across an entire water body. Thus to take advantage of the merits of these disparate approaches, an intensive *in-situ* sampling programme may be mounted concurrently with a satellite based assessment to validate the results of remote sensing and to provide additional data especially on factors that are difficult to observed directly from space and are therefore frequently overlooked in remote sensing applications such as changing biota and the chemical characteristics including nutrient levels.

Thus, we assert that an improved understanding of how *in-situ* generated water quality data relate to remotely sensed data over time provides the necessary framework for development of remotely sensed water quality indicators. Such indicators may then be monitored using space-based measurements and be easily related to characteristics of the environment not directly

observable from space (Koponen et al. 2002). Currently, direct measurement of nutrient concentrations in tropical inland water bodies is an existing challenge for the remote sensing community (Dörnhöfer and Oppelt 2016). Most previous remote sensing studies focused on modeling chlorophyll-*a* at the expense of physico-chemical variables that are essential for phytoplankton growth namely phosphorus, nitrates and ammonia (Tyler et al. 2006, Wang et al. 2006, Lepisto et al. 2010, Karakaya et al. 2011, Song et al. 2011, Dube et al. 2015). The detection of high nutrient concentrations in a reservoir system using remote sensing can be valuable for future monitoring of water quality dynamics for sustainable water resources management. The aim of this study are to determine the relationships between nutrient concentrations and reflectance; and to test whether the relationships are stable over time as a preamble to the development of an operational an early warning system for water quality degradation based on satellite remote sensing. To this end, water quality samples were repeatedly collected from a Zimbabwean reservoir over six months to measure concentrations of nitrates, reactive phosphorus and ammonia. The field observations were then related to optical satellite data retrieved from Landsat OLI.

Materials and Methods

In-situ Water Quality Measurements

The utility of satellite remote sensing for timeous assessment of water quality was tested in Mazvikadei reservoir located at latitude 17° 13.1′ south and longitude 30° 23.5′ east in northern Zimbabwe. As of June 2013, the inundated area was approximately 21 km² with a maximum depth of 26 m. Previous research has suggested that Mazvikadei has a healthy green algae and a

thriving population of zooplankton (Masundire 1992). Although, the catchment of Mazvikadei is relatively well-protected it is under threat from several anthropogenic activities such as artisanal chrome mining and commercial agriculture characterized by use of chemical fertilizers.

Insert Figure 1 here

To test whether satellite remote sensing can aid monitoring of nutrient concentrations, eight sampling sites were selected at random using a geographic information system and monitored from May-October 2015. This time period is constituted by the "cool dry season" and "the hot dry season", where the former is characterized by low temperatures $(0 - 23 \, {}^{\circ}\text{C})$ and almost no precipitation. The hot dry season in contrast, is characterized by warm temperatures (15 – 35 °C) but again there is none or very little precipitation (Gwitira et al. 2014). The coordinates of the sampling points were saved in a handheld global positioning receiver, which was used to locate them. At each sampling site, water was collected using an integrated tube sampler to a depth of 1 m from the surface and stored in 500 ml polythene bottles. Repeated sampling of the same sites was done between noon and 1400 hours local time to minimize variation associated with different bathymetric characteristics of the reservoir. The sampling dates were chosen in advance to make the Landsat 8 images synchronous with water sampling. Water samples were analyzed at the University of Zimbabwe Department of Biological Sciences laboratory for nitrates, reactive phosphorus and ammonia using standard methods described in Bartram and Ballance (1996). The minimum detectable value when measuring reactive phosphorus concentration using the solvent extraction procedure was 0.0005 mg/l while the minimum detectable value when measuring ammonia concentration using the salicylate method was 0,003 mg/l.

Remote Sensing Datasets

In this study, Landsat 8 OLI imagery with a spatial resolution of 30 m in the optical bands were downloaded from the United States Geological Survey (USGS) Earth Explorer website (www.earthexplorer.usgs.gov). A total of six Landsat images (path 170, row 72) acquired on 21 May, 11 June, 28 July, 27 August, 10 September and 30 October in 2015 were used in this study. All Landsat bands were atmospherically corrected using the Dark Object Subtraction method, and converted from DN values to radiances and then from radiances to top-of-atmosphere reflectance following a standard method that uses coefficients extracted from the header file (Chander et al. 2009) in Quantum GIS (version 2.10 Pisa).

A point map showing the location of each sampling point was generated and overlaid on top of the imagery to extract reflectance values of each bands at these points. The reflectance values for each band were then related with the physico-chemical variables at each of the sampling points. At each sample station, the average reflectance value for a 3 x 3 window centered on these pixels was calculated to generate a satellite-based "sample" that corresponded with a ground-based sample (Olmanson et al. 2011). This spatial window was used to account for potential locational errors caused by GPS as well as due to boat drift.

Relating In-Situ Nutrient Concentrations to Satellite Data

To assess the nature and strength of the relationships, the reflectance values of the single bands, that is the blue (450-510 nm), green (530-590 nm), red (640-670 nm), near infra-red (850-880 nm) and the Short Wave Infrared 1 (1570-1650 nm) were separately regressed against ammonia,

nitrates and reactive phosphorus concentrations measured *in-situ*. Different band ratios were also computed and regressed against observed data. The single band and the band ratios were the independent variables. The coefficient of determination (R^2) was used as a statistical measure of how successful the fitted regression model was in explaining the variation of the observed data. R^2 values range from 0 to 1, with values close to 1 indicating good model fit. We then applied regression models with an $R^2 \ge 0.66$, the lowest value to be accepted in regression analysis (Crawley 2002), to the respective Landsat 8 data to predict the spatial distribution of nutrient concentrations throughout the reservoir.

Results

Nutrient Concentrations

The average ammonia concentration measured in the reservoir was $0.0112 \ mgl^{-1}$. Ammonia concentrations were low and almost constant from May-October ranging from $0.009\text{-}0.034 \ mgl^{-1}$ (Table 1). However, in July there was a sharp increase at site 3 and slight increase at sites 5 and 6. Reactive phosphorus (RP) was highest in May for all the sites ranging from $0.045\text{-}0.12 \ mgl^{-1}$ (Table 1). The average concentration of RP in the reservoir was $0.019 \ mgl^{-1}$. The concentrations were almost constant from June to September varying slightly within a range of $0.0005\text{-}0.022 \ mgl^{-1}$. In July at site 3, the RP concentration rose to $0.022 \ mgl^{-1}$ but its concentration increased slightly in October to a range of $0.0095\text{-}0.023 \ mgl^{-1}$. The average nitrate concentration in the reservoir was $0.01 \ mgl^{-1}$. Nitrate concentrations fluctuated from May-August within a range of $0.0006\text{-}0.028 \ mgl^{-1}$ (Table 1). The concentrations decreased for most of the sites from September-October to concentrations of $0.0026\text{-}0.09 \ mgl^{-1}$.

Insert Table 1 here

Relationships between Nutrient Concentrations and Single Band Reflectance

The relationship between nutrient concentrations and reflectance for both the single bands was not stable but varied from month to month throughout the sampling period as shown in Tables 2 to 4. Specifically, the strongest relationship was observed between ammonia and reflectance with an $R^2 = 0.79$ (Table2; Figure 2). The near-infrared also displayed the strongest relationship with reactive phosphorus ($R^2 = 0.47$) during the month of June (Table 3) but the fitted model could only explain less than 50% of the variation in RP. The relationship between nitrates and the blue band was highest in July ($R^2 = 0.67$) as summarized in Table 4 and graphed in Figure 3.

Insert Figure 2 here

Insert Figure 3 here

Insert Table 2, Table 3 and Table 4 here

Relationships between Nutrient Concentrations and Band Ratios

The highest R^2 value for ammonia was obtained for the ratio of reflectance in the Red to the Blue in June. During other months, the relationship was weak and statistically insignificant. There was no significant relationship between reactive phosphorus and the different band ratio combinations throughout the study period from May-October 2015 (Table 5). In contrast, a significant relationship was observed for nitrates and the ratio of Shortwave infrared to red ($R^2 = 0.51$) in June. Generally, the R^2 values for the nitrates and other band ratios were highest in May

9

(Table 6) but comparatively these values were lower than those observed for single bands in July (see Table 4). A general observation that can be made from Tables 5 to 7 is that two band ratios, that is, the Red to Blue and SWIR-1 to NIR are promising for monitoring ammonia and nitrates in Mazvikadei, respectively.

Insert Table 5 here

Insert Table 6 here

Insert Table 7 here

Spatial Prediction of Nutrient Concentrations

Figure 4 shows the distribution of ammonia concentration in Mazvikadei generated by applying the regression model shown in Figure 2 to the near infrared red band of Landsat 8 of 11 June 2015. The results in Figure 4 show that ammonia was uniformly distributed throughout the reservoir. The results further show that much of the ammonia concentration is found along the edges of the reservoir. A different pattern was observed for nitrates. Figure 5 shows that the nitrates were concentrated more on the western areas of the reservoir, which borders commercial farms associated with high use of inorganic fertilizers in comparison to other areas. The nitrate concentration map was derived from applying the regression equation shown in Figure 3 to the blue band of Landsat 8 of 28 July 2015.

Discussion

The results of this study indicate that the relationship between reflectance derived from Landsat 8 and nutrients in a subtropical reservoir was not stable but changed with time. During the month

of July, the NIR followed by the green bands was significantly related to ammonia in Mazvikadei. However, for other months, the relationship was weak and insignificant. These results suggest that the midst of the cool dry season may be an important period for detecting nutrient concentrations in Mazvikadei using satellite remote sensing in the optical domain.

Another important aspect of the results is that the blue band could explain 67% of the variation in nitrates in Mazvikadei during the month of June. These results agree with previous studies that have observed time-dependency in the relationship between reflectance and other water quality parameters that are amenable to remote sensing such as chlorophyll-a (Wu and Cheng 2010, Li et al. 2011, Chawira et al. 2013). However, this may be the first time such relationships have been documented for nitrates and ammonia in African reservoirs using medium resolution multi-spectral sensors such as Landsat 8.

From the instability of the relationship between nutrients and reflectance over time, one may deduce that there exists a narrow window of opportunity especially during the cool dry season within which satellite remote sensing may be deployed to give a realistic picture of nutrient concentrations that mirrors *in-situ* conditions. With regard to ammonia and nitrates, the months of June and July were the most promising to assess and monitor these nutrients concentrations remotely. The explanation for why these particular months showed significant relationships with satellite reflectance are not yet clear, but it may be that during the cool dry season, these two nutrients will be almost evenly distributed throughout the water column soon after turnover occurs. However, this inference needs to be interpreted with caution since the study was done in one reservoir.

In contrast to the cool dry season, nutrient concentrations fluctuate a lot during the hot season thus rendering remote sensing less useful for monitoring nutrients in subtropical reservoirs. It has been suggested recently that in relatively small tropical reservoirs such as the one studied here, the concentrations of nitrogen tend to increase during the hot wet season because of various forms of runoff that wash nitrates from the catchment into the water body (Dalu et al. 2015). Additional nitrogen may also be released into the air due to ammonia volatization. Atmospheric deposition in the form of acid rain can also affect nutrient concentration in water (Paerl 1997). The increases in nitrates may also be due to sediment particles that tend to be re-suspended during the rainy season and this in turn increases nitrate loads in the reservoir.

While it is well established that water constituents such as the nutrients affect the absorption and scattering properties of incoming light (Dekker et al. 1996) and thus potentially changing the spectral properties of a reservoir, our work may be the first to report a significant relationship between nitrates and the ratio of reflectance in the short wave to red bands during the month of May in a subtropical African reservoir. This relationship needs to be explored further as most previous studies have only explored the use of the red, green and near infrared bands to assess water quality (Han and Jordan 2005, Cannizzaro and Carder 2006, Dalu et al. 2015).

An interesting feature of the results is that reflectance was not significantly related to reactive phosphorus (RP) regardless of whether single or band ratios were used. In addition, repeating the analysis in different months spread over different seasons, did not change the results. From this finding, one may deduce that RP is not amenable to detection using multi-spectral remote sensing especially in the optical domain. Part of the explanation may be because Mazvikadei is

an oligotrophic reservoir characterized by low N and P levels (Masundire 1992). This implies the use of remote sensing in determining nutrient status of tropical reservoirs may therefore be more effective for mesotrophic and eutrophic reservoirs but further research is needed before any conclusions can be drawn.

Where our approach differs from previous studies is in testing the strength of the relationship between three nutrients and reflectance derived from the recently launched Landsat 8 over three different seasons in a tropical African reservoir. Most remote sensing applications for water quality assessment target parameters such as chlorophyll-a and transparency that are easy to detect directly using remote sensing and yet for Water Quality Management, these are normally end points signifying that water quality has deteriorated such that when they are detected it may already be too late to intervene. By repeatedly sampling water from the same sample points over different seasons and relating *in-situ* nutrient concentrations with Landsat 8 retrieved reflectance we were able to demonstrate the cool dry season as ideal for monitoring ammonia and nitrate concentrations using multi-spectral remote sensing. This result suggests that the freely and readily available Landsat 8 datasets are useful for developing an operational system for monthly monitoring of nutrient concentrations in standing water bodies in Africa. However, it has to be acknowledged that the revisit time of Landsat is 16 days. This is longer than that of other satellite datasets such as MERIS with a revisit time of 2-3 days making daily monitoring of water quality using Landsat 8 impossible. But, in the optical domain, Landsat 8 has a higher spatial resolution of 30 m. This is particularly important in the African context where most reservoirs are small (< 1 km² in area). In contrast, the spatial resolution of MERIS and MODIS with short revisit time makes these sensors ideal for large water bodies only (Matthews et al. 2010).

From a remote sensing perspective, a limitation of the present study is that the effect of suspended sediments or colored dissolved organic matter on the remotely sensed retrieved measurements was not taken into account during the analysis. In addition, noise originating from atmospheric sources such as haze could have altered the relationship between nutrient concentrations and reflectance during the hot dry season. Nevertheless, the results seem robust since relationships were explored over six months spread over three different seasons.

Conclusion

The utility of Landsat 8 for assessing nutrient concentrations was tested with the datasets of water samples collected from a subtropical reservoir in Zimbabwe. Overall, the results demonstrate that Landsat 8, which is available in the public domain, is useful for detecting nutrient concentrations especially ammonia and nitrates in subtropical inland reservoirs during the cool dry season. The approach described in the present work can be applied in other reservoirs elsewhere in the subtropics with the aim to detecting narrow windows of opportunity, most likely during the cool dry season, in which nutrient concentrations may be monitored remotely using multispectral data.

References

Bartram, J. and R. Ballance. 1996. (Eds) Water Quality Monitoring: A Practical Guide to the Design of Freshwater Quality Studies and Monitoring Programme. UNEP/WHO, Chapman & Hall, London.

Binding, C. E., T. A. Greenberg, and R. P. Bukata. 2012. An analysis of MODIS-derived algal and mineral turbidity in Lake Erie. Journal of Great Lakes Research **38**:107-116.

- Cannizzaro, J. P. and K. L. Carder. 2006. Estimating chlorophyll-*a* concentrations from remotesensing reflectance in optically shallow waters. Remote Sensing of Environment **101**:13-24.
- Chander, G., B. L. Markham, and D. L. Helder. 2009. Summary of current radiometric calibration coefficients for Landsat MSS, TM, ETM+, and EO-1 ALI sensors. Remote Sensing of Environment 113:893-903.
- Chawira, M., T. Dube, and W. Gumindoga. 2013. Remote sensing based water quality monitoring in Chivero and Manyame lakes of Zimbabwe. Physics and Chemistry of the Earth **66**:38-44.
- Crawley, M. J. 2002. Statistical computing: an introduction to data analysis using SPLUS. John Wiley Chichester.
- Dalu, T., T. Dube, P. W. Froneman, M. T. B. Sachikonye, B. W. Clegg, and T. Nhiwatiwa. 2015.

 An assessment of chlorophyll-a concentration spatiotemporal variation using Landsat satellite data, in a small tropical reservoir. Geocarto International **30**:1130-1143.
- Dekker, A. G., Z. Zamurovic-Nenad, H. J. Hoogenboom, and S. W. M. Peters. 1996. Remote sensing, ecological water quality modeling and in situ measurements: a case study in shallow lakes. Hydrological Sciences **41**:531-549.
- Dörnhöfer, K. and N. Oppelt. 2016. Remote sensing for lake research and monitoring Recent advances. Ecological Indicators **64**.
- Duan, H., Y. Zhang, B. Zhang, K. Song, and Z. Wang. 2007. Assessment of chlorophyll-a concentration and trophic state for Lake Chagan using Landsat TM and field spectral data. Environment and Natural Resources Research 2:295-308.

- Dube, T., O. Mutanga, K. Seutloali, S. Adelabu, and C. Shoko. 2015. Water quality monitoring in sub-Saharan African lakes: a review of remote sensing applications. African Journal of Aquatic Science **40**:1-7.
- Ekstrand, S. 1992. Landsat TM based quantification of chlorophyll-*a* during algae blooms in coastal waters. International Journal of Remote Sensing **13**:1913-1926.
- Gordoa, A., X. Illas, A. Cruzado, and Z. Velasquez. 2008. Spatio-temporal patterns in the North-Western Mediterranean from MERIS derived chlorophyll a concentration. Scientia Marina **72**:757-767.
- Gwitira, I., A. Murwira, M. D. Shekede, M. Masocha, and C. Chapano. 2014. Precipitation of the warmest quarter and temperature of the warmest month are key to understanding the effect of climate change on plant species diversity in Southern African savannah. African Journal of Ecology **52**:209-216.
- Han, L. and K. J. Jordan. 2005. Estimating and mapping chlorophyll-a concentration in Pensacola Bay, Florida using Landsat ETM+ data. International Journal of Remote Sensing **26**:5245-5254.
- Karakaya, N., F. Evrendilek, G. Aslan, K. Gungor, and D. Karakas. 2011. Monitoring of lake water quality along with trophic gradient using landsat data. International Journal of Environmental Science and Technology 8:817-822.
- Koponen, S., J. Pulliainen, K. Kallio, and M. Hallikainen. 2002. Lake water quality classification with airborne hyper spectral spectrometer and simulated MERIS data. Remote Sensing of Environment **79**:51-59.

- Lepisto, A., T. Huttula, S. Koponen, K. Kallio, A. Lindfors, M. Tarvainen, and J. Sarvala. 2010.

 Monitoring of spatial water quality in lakes by remote sensing and transect

 measurements. Aquatic Ecosystem Health & Management 13:176-184.
- Li, L., L. Li, K. Song, Y. Li, K. Shi, and Z. Li. 2011. An improved analytical algorithm for remote estimation of chlorophyll-*a* in highly turbid waters. Environmental Research Letters **6** (3): 34037-34043.
- Masundire, H. M. 1992. The filling phase of Mazvikadei reservoir, Zimbabwe. Hydrobiologia **23**:11-17.
- Matthews, M. W. 2014. Eutrophication and cyanobacterial blooms in South African inland waters: 10 years of MERIS observations. Remote Sensing of Environment **155**:161-177.
- Matthews, M. W., S. Bernard, and K. Winter. 2010. Remote sensing of cyanobacteria-dominant algal blooms and water quality parameters in Zeekoevlei, a small hypertrophic lake, using MERIS. Remote Sensing of Environment 114:2070-2087.
- Moore, G. K. 1980. Satellite remote sensing of water turbidity. Hydrological Sciences **25**:407-421.
- Ndungu, J., B. C. Monger, D. C. M. Augustijn, S. J. M. H. Hulscher, N. Kitaka, and J. M. Mathooko. 2013. Evaluation of spatio-temporal variations in chlorophyll-a in Lake Naivasha Kenya: remote-sensing approach. International Journal of Remote Sensing 34:8142-8155.
- O'Reilly, J. E., S. Maritorena, B. G. Mitchell, D. A. Siegel, K. L. Carder, S. A. Garver, M. Kahru, and C. Mcclain. 1998. Ocean Color Chlorophyll Algorithms for SeaWiFS. Journal of Geophysical Research 103:24937-24953.

- Olmanson, L. G., P. L. Brezonik, and M. E. Bauer. 2011. Evaluation of medium to low resolution satellite imagery for regional lake water quality assessments. Water Resources Research 47:1-14.
- Paerl, H. W. 1997. Coastal eutrophication and harmful algal blooms: Importance of atmospheric deposition and groundwater as" new" nitrogen and other nutrient sources. Limnology and Oceanography **42**:1154-1165.
- Skidmore, A. K., B. Witske, K. Schmidt, and L. Kumar. 1997. Use of Remote sensing and GIS for sustainable land management. ITC Journal 3:302-315.
- Song, K. S., Z. M. Wang, J. Blackwell, B. Zhang, F. Li, Y. Z. Zhang, and G. J. Jiang. 2011.

 Water quality monitoring using Landsat Themate Mapper data with empirical algorithms in Chagan Lake, China. Journal of Applied Remote Sensing 5:053506-053516.
- Tyler, A. N., E. Svab, T. Preston, M. Presing, and W. A. Kovacs. 2006. Remote sensing of the water quality of shallow lakes: A mixture modelling approach to quantifying phytoplankton in water characterized by high-suspended sediment. International Journal of Remote Sensing 27:1521-1537.
- Usali, N. and M. H. Ismail. 2010. Use of remote sensing and GIS in monitoring water quality.

 Journal of Sustainable Development 3:228-239.
- Wang, F., L. Han, H. T. Kung, and R. B. van Arsdale. 2006. Applications of Landsat-5 TM imagery in assessing and mapping water quality in Reelfoot Lake, Tennessee.

 International Journal of Remote Sensing 27:5269-5283.
- Wu, X. J. and Q. A. Cheng. 2010. Estimation of chlorophyll a and total suspended matter concentration using Quickbird image and in situ spectral reflectance in Hangzhou Bay,

China. *In* C. M. U. Neale and A. Maltese, editors. Remote Sensing for Agriculture, Ecosystems, and Hydrology Xii.

Table 1. Descriptive statistics for nutrient concentration levels measured at eight sample sites in Mazvikadei reservoir for the period May – October 2015

| | | | | | | | | | | | | |)) | | | |
|--------------|------|-----|------|-----|------|-----|------|-----|------|-----|------|------------|------|-----|------|------|
| | site | | site | | site | | site | | site | | site | >// | site | | site | |
| | 1 | | 2 | | 3 | | 4 | | 5 | ^ | 6 | \bigcirc | 7 | | 8 | |
| Nutrient | Me | SD | Me | SD | Me | SD |
| | an | | an | | an | | an | _ | an | 7 | an | | an | | an | |
| AMM | 0.0 | 0.0 | 0.0 | 0.0 | 0.0 | 0.0 | 0.0 | 0.0 | 0.0 | 0.0 | 0.0 | 0.0 | 0.0 | 0.0 | 0.0 | 0.00 |
| (mgl^{-1}) | 146 | 099 | 116 | 026 | 107 | 016 | 105 | 007 | 103 | 004 | 104 | 009 | 107 | 004 | 106 | 04 |
| RP | 0.0 | 0.0 | 0.0 | 0.0 | 0.0 | 0.0 | 0.0 | 0.0 | 0.0 | 0.0 | 0.0 | 0.0 | 0.0 | 0.0 | 0.0 | 0.02 |
| (mgl^{-1}) | 207 | 220 | 147 | 220 | 187 | 228 | 314 | 437 | 175 | 225 | 116 | 174 | 199 | 293 | 173 | 69 |
| NITR | 0.0 | 0.0 | 0.0 | 0.0 | 0.0 | 0.0 | 0.0 | 0.0 | 0.0 | 0.0 | 0.0 | 0.0 | 0.0 | 0.0 | 0.0 | 0.00 |
| (mgl^{-1}) | 210 | 340 | 119 | 095 | 064 | 040 | 092 | 052 | 062 | 041 | 053 | 035 | 115 | 083 | 088 | 70 |

N.B: AMM = Ammonia, RP = Reactive Phosphorus, NITR = Nitrate, SD stands for standard deviation calculated from six observations per sampling site.

Table 2. R² values indicating the strength of the relationship between single bands and ammonia

| Band | | | | | |
|-------------------|----------|--------|-------|----------|--------|
| Date | Red | Blue | Green | NIR | SWIR 1 |
| 21 May 2015 | 0.038 | 0.040 | 0.07 | 3.00E-05 | 0.014 |
| 11 June 2015 | 0.510 | 0.410 | 0.718 | 0.799 | 0.490 |
| 28 July 2015 | 0.003 | 0.050 | 0.090 | 0.056 | 0.009 |
| 27 August 2015 | 0.008 | 0.020 | 0.050 | 0.042 | 0.007 |
| 10 September 2015 | 7.00E-05 | 0.0003 | 0.002 | 0.001 | 0.007 |
| 30 October 2015 | 0.080 | 0.070 | 0.080 | 0.058 | 0.071 |

SWIR 1 = Short Wave Infra Red, NIR=Near Infra Red

Values in bold face indicate significant relationships (P < 0.05).

Table 3. R² values indicating the strength of the relationship between single bands and reactive phosphorus

| Band | | | | | |
|-------------------|-------|----------|----------|-------|-------|
| Date | Red | Blue | Green | NIR | SWIR |
| 21 May 2015 | 0.23 | 0.270 | 0.280 | 0.010 | 0.070 |
| 11 June 2015 | 0.15 | 0.314 | 0.366 | 0.470 | 0.438 |
| 28 July 2015 | 0.02 | 0.208 | 0.282 | 0.065 | 0.002 |
| 27 August 2015 | 0.08 | 0.008 | 3.00E-06 | 0.005 | 0.076 |
| 10 September 2015 | 0.003 | 4.00E-07 | 0.010 | 0.007 | 0.001 |
| 30 October 2015 | 0.05 | 0.046 | 0.059 | 0.049 | 0.053 |

Values in bold indicate significant relationship (P < 0.05).

Table 4. R² values indicating the strength of the relationship between single bands and nitrates

| Band | | | | | |
|-------------------|-------|-------|-------|-------|--------|
| Date | Red | Blue | Green | NIR | SWIR 1 |
| 21 May 2015 | 0.396 | 0.326 | 0.316 | 0.482 | 0.281 |
| 11 June 2015 | 0.001 | 0.005 | 0.192 | 0.044 | 0.021 |
| 28 July 2015 | 0.071 | 0.672 | 0.618 | 0.246 | 0.134 |
| 27 August 2015 | 0.189 | 0.083 | 0.105 | 0.096 | 0.019 |
| 10 September 2015 | 0.177 | 0.207 | 0.278 | 0.178 | 0.134 |
| 30 October 2015 | 0.472 | 0.401 | 0.410 | 0.401 | 0.469 |

Values in bold face indicate significant relationships (P < 0.05).

Table 5. R² values for relationship between different band ratios and ammonia

| Band ratio | | | | | |
|-------------------|----------|------------|----------|------------|-------------|
| Date | NIR/ Red | Red/ Green | Red/Blue | SWIR 1/NIR | SWIR 1/ Red |
| 21 May 2015 | 0.053 | 0.0003 | 0.039 | 0.030 | 0.047 |
| 11 June 2015 | 0.409 | 0.473 | 0.508 | 0.342 | 0.018 |
| 28 July 2015 | 0.016 | 0.010 | 0.009 | 0.0006 | 0.250 |
| 27 August 2015 | 0.066 | 0.019 | 0.020 | 0.097 | 0.020 |
| 10 September 2015 | 0.012 | 3.00E-07 | 0.0002 | 0.034 | 0.015 |
| 30 October 2015 | 0.037 | 0.058 | 0.051 | 0.049 | 0.084 |

Values in bold indicate significant relationship (P < 0.05).

Table 6. R² values for relationship between different band ratios and reactive phosphorus

| Band ratio | | | | | |
|-------------------|----------|------------|----------|------------|-------------|
| Date | NIR/ Red | Red/ Green | Red/Blue | SWIR 1/NIR | SWIR 1/ Red |
| 21 May 2015 | 6.00E-05 | 0.054 | 0.186 | 0.099 | 0.036 |
| 11 June 2015 | 0.050 | 0.123 | 0.132 | 0.362 | 0.193 |
| 28 July 2015 | 0.047 | 0.041 | 0.045 | 0.013 | 0.371 |
| 27 August 2015 | 0.126 | 0.108 | 0.111 | 0.182 | 0.116 |
| 10 September 2015 | 0.046 | 0.005 | 0.008 | 0.017 | 0.036 |
| 30 October 2015 | 0.033 | 0.045 | 0.048 | 0.061 | 0.006 |

SWIR 1=Short Wave Infra Red, NIR=Near Infra Red.

Table 7. R² values for relationship between different band ratios and nitrates

| Band ratio | | | | | |
|-------------------|----------|------------|-----------|------------|-------------|
| Date | NIR/ Red | Red/ Green | Red/ Blue | SWIR 1/NIR | SWIR 1/ Red |
| 21 May 2015 | 0.429 | 0.499 | 0.430 | 0.533 | 0.554 |
| 11 June 2015 | 0.042 | 0.001 | 0.002 | 0.011 | 0.132 |
| 28 July 2015 | 0.057 | 0.031 | 0.020 | 0.072 | 0.012 |
| 27 August 2015 | 0.005 | 0.012 | 0.012 | 9.00E-05 | 0.024 |
| 10 September 2015 | 0.151 | 0.161 | 0.162 | 0.099 | 0.201 |
| 30 October 2015 | 0.398 | 0.463 | 0.465 | 0.497 | 0.257 |

Values in bold indicate significant relationship (P < 0.05).

Figure Captions

Figure Error! No text of specified style in document. Location map of Mazvikadei reservoir in the northeastern region of Zimbabwe showing distribution of sampled points from May-October 2015. The units for axes are meters based on the Universal Tranverse Mercator projection, zone 36K South with the WGS 84 as the datum.

Figure 2: Relationship between ammonia concentration and reflectance in the near infrared band of Landsat 8 in Mazvikadei reservoir of Zimbabwe. The Landsat 8 OLI image was acquired on 11 June 2015.

Figure 3: Scatterplot showing the relationship between concentration of nitrates and reflectance in the Landsat 8 blue band in Mazvikadei reservoir in Zimbabwe. The Landsat 8 image OLI was acquired on 28 July 2015.

Figure 4: Spatial distribution of ammonia concentrations in Mazvikadei reservoir on 11 June 2015 derived from applying a linear regression equation to the near infrared band of Landsat 8 satellite data. The units for axes are meters based on the Universal Tranverse Mercator projection, zone 36K South with the WGS 84 as the datum.

Figure 5: Spatial distribution of the concentration of nitrates in Mazvikadei reservoir on 28 July 2015 generated by applying a linear regression equation the blue band of Landsat 8 satellite data. The units for axes are meters based on the Universal Tranverse Mercator projection, zone 36K South with the WGS 84 as the datum.

